

## Synthesis of Novel Push–Pull Chromophores based on *N*-Ethylcarbazole for Vacuum Deposition Processed Organic Photovoltaics

Takahiro Kono,<sup>1,2</sup> Yosei Shibata,\*<sup>1</sup> Zhiping Wang,<sup>1</sup> Tetsuhiko Miyadera,<sup>1,3</sup> and Yuji Yoshida\*<sup>1</sup>

<sup>1</sup>Research Center for Photovoltaic Technologies, National Institute of Advanced Industrial Science and Technology (AIST), Central 5, 1-1-1 Higashi, Tsukuba, Ibaraki 305-8565

<sup>2</sup>Center for Energy and Environmental Science, Shinshu University, 3-15-1 Tokida, Ueda, Nagano 386-8567

<sup>3</sup>PRESTO, Japan Science and Technology Agency (JST), 4-1-8 Honcho, Kawaguchi, Saitama 332-0012

(E-mail: yosei.shibata@aist.go.jp, yuji.yoshida@aist.go.jp)

Two novel p-type materials, Cz(Et)ThOM and Cz(Et)OM—respectively with and without a thiophene  $\pi$ -spacing unit—have been synthesized for vacuum-deposited organic photovoltaics (OPVs). The power conversion efficiencies of planar heterojunction OPVs of the former are clearly higher than that of the latter. Further improvement of the device with Cz(Et)ThOM was obtained by employing bulk heterojunction structure and post-annealing. The structural analysis of thin films by synchrotron X-ray diffraction and atomic force microscopy shows that this improvement is due to Cz(Et)ThOM becoming highly ordered during annealing.

Vacuum deposition has recently attracted much attention as a potential means to realize tandem-structured organic photovoltaic (OPV) devices with a wide absorbance for sunlight.<sup>1,2</sup> One of the advantages of organic semiconductor materials in this context is that the absorption range is controllable from ultraviolet/visible to near-infrared wavelengths. High-performance vacuum-deposited OPVs need to be achieved with small molecules. Therefore, to obtain enhanced performance, novel electron donor materials in OPVs are required with high molar absorption coefficients ( $\epsilon$ ) for long wavelengths. For OPV applications, electron donor materials should have narrow energy gaps between their highest occupied and lowest unoccupied molecular orbitals (HOMO and LUMO, respectively). On the other hand, a deep HOMO level is also important because the open-circuit voltage ( $V_{oc}$ ) in OPV devices strongly depends on the difference between the HOMO of the donor and the LUMO of the acceptor.<sup>3</sup> Furthermore, in view of vacuum fabrication, the thermal stability of the material is crucial. To date, however, the literature on small molecules for vacuum-deposited OPV devices is sparse.

To synthesize small molecules that satisfy the above-mentioned requirements, we focused on push–pull chromophores with an asymmetric structure. Push–pull chromophores based on a donor– $\pi$ -spacer–acceptor (D– $\pi$ –A) structure offer potentially high  $\epsilon$  values, making them attractive candidates for high-performance OPV applications.<sup>4–8</sup> In addition, their light absorption properties and HOMO–LUMO levels are readily controllable via structural modifications of the electron donor and acceptor moieties. In spite of these advantages, however, an optimal molecular design based on push–pull chromophores with a  $\pi$ -spacer for OPV devices has not been firmly established till date. As donor and acceptor skeletons, respectively, we chose *N*-ethylcarbazole and 2-(3-oxoindene)malononitrile, the latter possessing two cyano and one ketone substituents with strong electron-accepting properties. The carbazole unit affords high

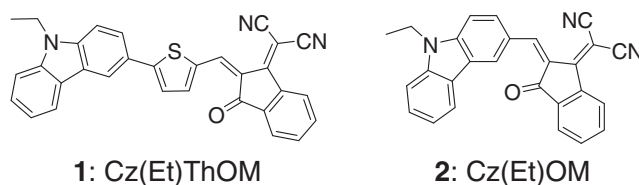


**Figure 1.** The molecular structure of Cz(Et)ThOM and Cz(Et)OM.

power conversion efficiency of up to 9% in dye-sensitized solar cells with the MK dye<sup>9–11</sup> and a hole mobility of  $0.1 \text{ cm}^2 \text{ V}^{-1} \text{ s}^{-1}$  in indolocarbazole organic field effect transistors.<sup>12</sup> The electron-donating property and steric planar structure of the carbazole unit clearly contributed to these results. However, a smaller structure would be preferable for OPV applications to confer the thermal stability required for vacuum deposition. In small  $\pi$ -conjugated molecules, the intramolecular interactions between strong donor and acceptor units can narrow the HOMO–LUMO gap and afford long-wavelength absorption, while a strong acceptor unit also provides deep HOMO and LUMO levels.

Herein, we report the synthesis of, and the optical and electrochemical properties of the novel push–pull chromophores, Cz(Et)ThOM and Cz(Et)OM (hereafter referred to as compounds **1** and **2**; Figure 1). The performance of planar heterojunction OPV devices prepared with compound **1** being clearly superior, a more focused optimization was performed, revealing substantial improvements after preparation of a bulk heterojunction (BHJ: donor–acceptor blend) structure and thermal treatment. This paper focuses on the relationship between the OPV performance and crystallinity of Cz(Et)ThOM films, as revealed by synchrotron X-ray diffraction.

The synthesis of these compounds is described in the Supporting Information. Ultraviolet–visible absorption spectra were recorded to investigate their photophysical and electrochemical properties, with absorption maxima and  $\epsilon$  in a tetrahydrofuran solution observed at 572 nm ( $\epsilon = 45400 \text{ M}^{-1} \text{ cm}^{-1}$ ) and 514 nm ( $\epsilon = 33900 \text{ M}^{-1} \text{ cm}^{-1}$ ) for compounds **1** and **2**, respectively. The molar absorbance coefficient of compound **1** is higher than that of **2** and its absorption peak is red-shifted compared with **2**. These results are ascribed to the extended  $\pi$ -conjugation that results from the insertion of the electron-donating thiophene ring. The HOMO level energies of thin films of the two materials were measured by photoelectron yield spectroscopy, giving 5.78 and 5.94 eV, respectively. This suggests that OPV devices prepared with compound **1** or **2** as the donor material will have a large  $V_{oc}$ , since as mentioned above, this strongly depends on the difference between the HOMO and

**Table 1.** Parameters from  $J$ - $V$  measurements on planar heterojunction devices prepared with compound **1** or **2**

Device <sup>a</sup>	$J_{sc}$ /mA cm <sup>-2</sup>	$V_{oc}$ /V	Fill factor	PCE /%
<b>1</b> ( $D_1 = 15$ nm)	3.57 ± 0.10	1.03 ± 0.02	0.44 ± 0.02	1.61 ± 0.07
<b>1</b> ( $D_1 = 30$ nm)	2.86 ± 0.17	1.06 ± 0.00	0.42 ± 0.01	1.27 ± 0.10
<b>2</b> ( $D_1 = 15$ nm)	0.04 ± 0.01	0.61 ± 0.01	0.24 ± 0.00	0.01 ± 0.00
<b>2</b> ( $D_1 = 30$ nm)	0.04 ± 0.00	0.77 ± 0.01	0.21 ± 0.00	0.01 ± 0.00

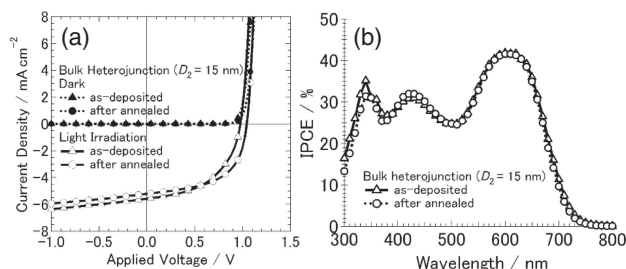
<sup>a</sup>Device area: 0.04 cm<sup>2</sup>.

LUMO levels of the donor and acceptor materials, respectively (The LUMO level of fullerene C<sub>60</sub> is ca. 4.5 eV).<sup>13</sup> The LUMO levels in these materials were estimated from their HOMO levels and the end-absorption of the thin films, giving 4.06 and 3.97 eV for **1** and **2**, respectively.

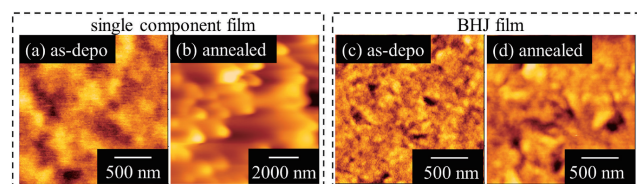
Organic photovoltaic devices were fabricated by vacuum deposition. The configuration of the planar heterojunction devices was as follows (with the thickness of each layer in parentheses): indium tin oxide (ITO)/MoO<sub>x</sub> (15 nm)/**1** or **2** (thickness  $D_1 = 15$  or 30 nm)/C<sub>60</sub> (50 nm)/Bathocuproine (BCP, 6 nm)/Al (100 nm). Table 1 and Supporting Information Figure S2a highlight the superior photovoltaic characteristics of device **1**, which has a  $V_{oc}$  greater than 1.0 V and higher incident photon-to-current efficiency (IPCE) and power conversion efficiency (PCE) than device **2** (see Figure S2 in the Supporting Information). To identify the origin of these differences, we calculated the series resistance ( $R_s$ , the internal resistance of the device) and the parallel resistance ( $R_p$ , due to current leakage in the device) by fitting the  $J$ - $V$  curves according to the Shockley diode model,<sup>14,15</sup> yielding  $R_s$  and  $R_p$  of 0.4 Ω cm<sup>2</sup> and 16.8 kΩ cm<sup>2</sup>, respectively, for device **1**, and 1.8 Ω cm<sup>2</sup> and 11.9 kΩ cm<sup>2</sup>, respectively, for device **2**. Although no differences in morphology or crystallinity were apparent between the two films, these values imply that the carrier transport property of compound **2** is poor.

The following discussion concerns compound **1**. To further improve the OPV performance, we prepared BHJ devices by coevaporation. The BHJ-type devices had the following configuration (with the thickness of each layer in parentheses) ITO/MoO<sub>x</sub> (15 nm)/**1** (5 nm)/**1**:C<sub>60</sub> = 1:1 v/v% (thickness  $D_2 = 15, 30,$  or 40 nm)/C<sub>60</sub>(50 nm)/BCP (6 nm)/Al (100 nm). The  $J$ - $V$  characteristics and IPCE spectra of these devices are shown in Figures 2a and 2b, respectively. Compared with the planar-type configuration, the BHJ configuration leads to an improved  $J_{sc}$ . This is attributed to the larger interface area between **1** and C<sub>60</sub>. The PCE of these devices were further improved by annealing treatment. The photovoltaic parameters of these BHJ devices are summarized in Table 2. The PCEs obtained are as high as ca. 3%. The  $J_{sc}$  and fill factor (FF) in a 15-nm and a 30-nm BHJ layer OPV are in a trade-off relationship. With a 40-nm-thick layer, both  $J_{sc}$  and the FF are reduced. Thermal treatment improves  $V_{oc}$  and the FF. The dark current of annealed devices was smaller than that of as-deposited devices as shown in Figures 2 and S3a. From these results, the improvement of  $V_{oc}$  was caused by the fact that carrier recombination loss was decreased by annealing treatment.

In order to understand the improvements in OPV performance following annealing, atomic force microscopy (AFM), and grazing incidence wide-angle X-ray scattering (GIWAXS) utilizing synchrotron irradiation were performed on BHJ films

**Figure 2.** Characteristics of bulk heterojunction devices prepared with compound **1**: (a)  $J$ - $V$  curves recorded under 100 mW cm<sup>-2</sup> light irradiation with air mass 1.5 G and (b) incident photon-to-current spectra.**Table 2.** Parameters from  $J$ - $V$  measurements on bulk heterojunction devices prepared with compound **1**:C<sub>60</sub>

Device <sup>a</sup>	$J_{sc}$ /mA cm <sup>-2</sup>	$V_{oc}$ /V	Fill factor	PCE /%
$D_2 = 15$ nm <sup>b</sup>	5.44 ± 0.12	0.97 ± 0.02	0.51 ± 0.00	2.70 ± 0.08
$D_2 = 15$ nm <sup>c</sup>	5.11 ± 0.06	1.04 ± 0.01	0.56 ± 0.00	2.99 ± 0.09
$D_2 = 30$ nm <sup>b</sup>	6.58 ± 0.18	0.96 ± 0.02	0.38 ± 0.01	2.37 ± 0.01
$D_2 = 30$ nm <sup>c</sup>	6.81 ± 0.02	1.05 ± 0.01	0.41 ± 0.01	2.90 ± 0.01
$D_2 = 40$ nm <sup>b</sup>	5.75 ± 0.20	0.90 ± 0.02	0.34 ± 0.01	1.77 ± 0.01
$D_2 = 40$ nm <sup>c</sup>	5.90 ± 0.08	1.01 ± 0.01	0.36 ± 0.00	2.15 ± 0.06

<sup>a</sup>Device area: 0.04 cm<sup>2</sup>. <sup>b</sup>As-deposited. <sup>c</sup>After annealing at 130 °C for 10 min.**Figure 3.** Atomic force micrographs of (a, b) compound **1** and (c, d) **1**:C<sub>60</sub> = 1:1 films deposited onto ITO/MoO<sub>x</sub> substrates, (a, c) as deposited and (b, d) after annealing (130 °C for 10 min).

and on single-component films of compound **1**. Figure 3 shows the AFM images obtained for as-deposited and heat-treated samples. The root-mean-square (RMS) roughnesses of the single-component films before and after annealing are 0.55 and 62.6 nm, respectively, which is a 110-fold increase. Figure 3b shows the aggregation structures that grow on **1** in the BHJ film during annealing. A similar trend in the RMS roughness is observed for the BHJ film, with 0.89 and 1.76 nm measured before and after annealing, respectively.

Figure 4 shows the GIWAXS images and the corresponding intensity plots obtained for these films in the in-plane direction. Both as-deposited **1** and **1**:C<sub>60</sub> BHJ films have no diffraction patterns, implying that as-deposited films are amorphous. On the other hand, diffraction patterns in these films appeared after annealing treatment. In particular, a comparison of Figures 4a and 4b highlights the appearance of a highly-oriented structure during heat treatment. A strong peak along the  $q_{xy}$  axis is observed, which is attributed to a  $\pi$ - $\pi$  stacking structure (calculated  $d$ -spacing: 3.56 Å at  $q_{xy} = 1.76 \text{ \AA}^{-1}$ ).

In Figure 4e, diffraction peaks are observed in the data acquired for both films after annealing. For the single-component

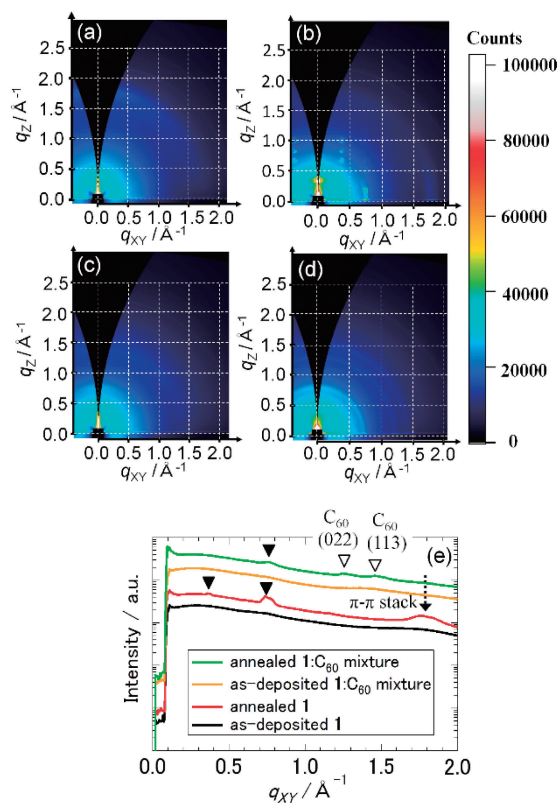


**Figure 4.** Grazing incidence wide-angle X-ray scattering images of (a, b) compound **1** and (c, d) **1**: $C_{60}$  = 1:1 films deposited onto ITO/ $MoO_x$  substrates, (a, c) as deposited and (b, d) after annealing (130 °C for 10 min), with (e) the corresponding  $q_{xy}$  intensity profiles.

film, the  $d$ -spacing values calculated from the peaks at  $q_{xy} = 0.36$  and  $0.75 \text{ \AA}^{-1}$  are 17.3 and  $8.7 \text{ \AA}$ , respectively, which are indicative of a highly ordered structure. Since the ring pattern was observed from GIWAXS measurement, annealed BHJ films show randomly oriented polycrystalline films. This suggests that the presence of fullerene hinders crystal growth in compound **1**. Nonetheless, the peak at  $q_{xy} = 0.75 \text{ \AA}^{-1}$  in Figure 4e shows that some crystallization of compound **1** occurs in the BHJ film with fullerene  $C_{60}$  during annealing. The two peaks at  $q_{xy} = 1.27$  and  $1.48 \text{ \AA}^{-1}$  are consistent with those that arise from the (022) and (113) planes of crystalline  $C_{60}$  with a face-centered-cubic lattice structure.<sup>16</sup> These results show that heat-treated **1**: $C_{60}$  = 1:1 BHJ films consist of randomly oriented crystals of compound **1** and  $C_{60}$ . Moreover, this comparative structural analysis of as-deposited and annealed films indicates that the molecules of compound **1** can be rearranged in an OPV cell by thermal treatment, leading to clear improvements in  $V_{oc}$  and the FF of the devices.

In summary, we have described the synthesis and characterization of two novel push-pull chromophores having  $N$ -ethylcarbazole and 2-(3-oxoindene)malononitrile as electron donor and acceptor units, respectively. These materials have a wide absorption range (400–650 nm) with a high molar absorption coefficient. The PCEs of OPV devices prepared with compound **1** (Figure 1) are clearly higher than those prepared with compound **2**, indicating that carriers are transported more efficiently in the former than in the latter. Annealing drastically

improves the  $V_{oc}$  and FF of devices based on compound **1**. The best PCE (ca. 3%) was obtained with a heat-treated BHJ device. From an analysis of film structure, this improvement was attributed to the increased crystallinity of compound **1** following annealing, which has a favorable effect on  $V_{oc}$  and FF.

This work has been supported by the Core Research for Evolutional Science and Technology (CREST) of the Japan Science and Technology Agency (JST). Synchrotron GIWAXS measurements were carried out at Spring-8 (beam line BL46XU, Japan) with the approval of JASRI (Nos. 2013A1629 and 2013A1781). We thank Dr. Tomoyuki Koganezawa (JASRI), Dr. Noboru Ohashi (AIST), and Ms. Hiroyo Usui (AIST) for advice on the GIWAXS measurements, valuable discussions, and support of this work.

Supporting Information is available electronically on J-STAGE.

## References

- X. Che, X. Xiao, J. D. Zimmerman, D. Fan, S. R. Forrest, *Adv. Energy Mater.* **2014**, *4*, 1400568.
- J. D. Zimmerman, B. E. Lassiter, X. Xiao, K. Sun, A. Dolocan, R. Gearba, D. A. Vanden Bout, K. J. Stevenson, P. Wickramasinghe, M. E. Thompson, S. R. Forrest, *ACS Nano* **2013**, *7*, 9268.
- M. C. Scharber, D. Mühlbacher, M. Koppe, P. Denk, C. Waldauf, A. J. Heeger, C. J. Brabec, *Adv. Mater.* **2006**, *18*, 789.
- S.-W. Chiu, L.-Y. Lin, H.-W. Lin, Y.-H. Chen, Z.-Y. Huang, Y.-T. Lin, F. Lin, Y.-H. Liu, K.-T. Wong, *Chem. Commun.* **2012**, *48*, 1857.
- L.-Y. Lin, Y.-H. Chen, Z.-Y. Huang, H.-W. Lin, S.-H. Chou, F. Lin, C.-W. Chen, Y.-H. Liu, K.-T. Wong, *J. Am. Chem. Soc.* **2011**, *133*, 15822.
- H. Bürckstümmer, E. V. Tulyakova, M. Deppisch, M. R. Lenze, N. M. Kronenberg, M. Gsänger, M. Stolte, K. Meerholz, F. Würthner, *Angew. Chem., Int. Ed.* **2011**, *50*, 11628.
- N. M. Kronenberg, V. Steinmann, H. Bürckstümmer, J. Hwang, D. Hertel, F. Würthner, K. Meerholz, *Adv. Mater.* **2010**, *22*, 4193.
- H. M. Ko, H. Choi, S. Paek, K. Kim, K. Song, J. K. Lee, J. Ko, *J. Mater. Chem.* **2011**, *21*, 7248.
- N. Koumura, Z.-S. Wang, S. Mori, M. Miyashita, E. Suzuki, K. Hara, *J. Am. Chem. Soc.* **2006**, *128*, 14256.
- N. Koumura, K. Hara, *Heterocycles* **2013**, *87*, 275.
- T. Uchiyama, T. N. Murakami, N. Yoshii, Y. Uemura, N. Koumura, N. Masaki, M. Kimura, S. Mori, *Chem. Lett.* **2013**, *42*, 453.
- H. Zhao, L. Jiang, H. Dong, H. Li, W. Hu, B. S. Ong, *ChemPhysChem* **2009**, *10*, 2345.
- P. Peumans, S. R. Forrest, *Appl. Phys. Lett.* **2001**, *79*, 126.
- S. Yoo, W. J. Potscavage, Jr., B. Domercq, S.-H. Han, T.-D. Li, S. C. Jones, R. Szoszkiewicz, D. Levi, E. Riedo, S. R. Marder, B. Kippeln, *Solid-State Electron.* **2007**, *51*, 1367.
- W. J. Potscavage, Jr., A. Sharma, B. Kippeln, *Acc. Chem. Res.* **2009**, *42*, 1758.
- E. V. Skokan, I. V. Arkhangelskii, D. E. Izotov, N. V. Chelovskaya, M. M. Nikulin, Y. A. Velikodnyi, *Carbon* **2005**, *43*, 803.